Journal of the Egyptian Mathematical Society
Journal homepage https://joems.journals.ekb.eg/
Print ISSN: 1110-256X Online ISSN: 2090-9128

http://dx.doi.org/10.21608/joems.2025.331474.1017

An Effective Mathematical Representation and Numerical Simulation for TB Prevention

Hoda A. Kamel, Hoda F. Ahmed, Rasha M. Farghly, Hala E. Abd El-Salam

Department of Mathematics, Faculty of Science, Minia University, Egypt.

Received: 2 Nov. 2024, Revised: 9 Jan. 2025, Accepted: 21 May 2025, Published online: 10 Oct. 2025

Abstract: The primary motivation of this research is to develop a realistic, non-linear mathematical model that accurately represents the transmission dynamics of tuberculosis (TB). Unlike existing models, this study incorporates a comprehensive analysis of key preventive measures, such as early detection, immunity, and personal hygiene, in mitigating the spread of TB bacteria. By explicitly modeling the impact of these factors, the research bridges a critical gap in understanding how public health measures, such as early detection, personal hygiene practices, and strong immunity, can substantially influence the course of infectious disease outbreaks. In addition, we aim with this study to develop a strategy to stop the spread of TB. The Shifted Chebyshev Spectral Collocation Technique (SCSC) has been used to obtain numerical results. The results obtained using the previously mentioned method show that as the immunity of community members improves, the number of recovered cases increases and the number of infected cases decreases. The results also made clear the importance of detecting the disease at the beginning of infection in order to prevent it and prevent the spread of infection, because the timing of diagnosis TB affects the speed of recovery and limits the spread of infection. The planned model consists of six epidemiological compartments. For the model, two steady-state points have been determined, one with and one without the pandemic. An endemic point EE is one that is present both locally and globally stable if $R_0 > 1$. The stability shows that the bacteria-free equilibrium (FE) is asymptotically stable both locally and globally for $R_0 < 1$. The model's sensitivity is assessed. We can apply such a mathematical model to many other infectious diseases.

Keywords: Non-linear mathematical model; Basic reproductive number; Stability analysis; Sensitivity analysis; SCSC Technique.

2020 AMS Subject Classifications: 54A05, 54C10, 54D10, 54D35, 91A05.

1 Introduction and Preliminaries

Numerous mathematical models [1–5] are employed to describe biological phenomena to comprehend the spread of the epidemic, its impacts, and how it was stopped and contained. One of the major problems of the modern period that has been seriously endangering human health in recent decades is TB [6] and [7]. Other articles that deal with the modelling can be found in [8, 9]. Frequent, long-term contact between healthy and infected individuals is the primary factor in the transmission of TB [10]. Tuberculosis (simply "TB") is an infectious disease that originally

* Corresponding author name and e-mail: Hala E. Abd El-Salam, hala.emad@mu.edu.eg

results from the bacterium TB. TB mainly affects the lungs (“pulmonary TB”) but is capable of attacking any body part (“extra pulmonary TB”).

TB was chosen as the focus of this study due to its significant global public health impact. TB remains one of the leading infectious diseases worldwide, causing millions of cases and deaths annually. Despite advances in treatment, TB continues to spread, especially in resource-limited settings, due to factors such as late diagnosis, limited access to healthcare, and the emergence of drug-resistant strains. By developing and analyzing a mathematical model for TB transmission. The spread of TB can be effectively prevented through early detection, immunity, and personal hygiene. Early detection, immunity, and personal hygiene are key factors in preventing the transmission of TB bacteria. Early detection allows for the identification and isolation of active cases, ensuring timely treatment that reduces infectiousness and breaks the chain of transmission. Strong immunity, supported by vaccination (e.g., BCG vaccine) and a healthy lifestyle, helps the body resist infection and prevent latent TB from becoming active. Personal hygiene, such as covering the mouth when coughing, maintaining good ventilation, and regular hand washing, minimizes the spread of TB bacteria in communities. Together, these measures effectively control TB and protect public health.

These models [11–13] are referred to as active epidemiological models and describe the long-term transmission and development of TB. They explain that before a person becomes infectious, the susceptible person goes through a latent phase after infection. In several published papers on TB transmission [14–16], it is shown that whether acquired immunity is permanent or not, it is of the ”SEIR” or ”SEIRS” type. Waaler and Anderson proposed the first TB model in 1962 [17]. ”SEIR” models that take density dependency in the death rate into account were examined by Greenhalgh [18]. SEIRS models with two delays were introduced and researched by Cooke and van den Driessche [19]. In recent years, Hopf bifurcations in SEIRS models with mortality rates have been examined by Greenhalgh [20]. The global dynamics of an SEIR model were examined by Zhang et al. [21]. The global dynamics of a bilinear incidence and vertical transmission SEIR model were reviewed by Li et al. [22]. Hai-Feng Huo and Ming-Xuan Zou Use a model to explain the importance of hospital treatment [23]. A system was designed to examine the effect of heterogeneity on how TB spreads by Okuonghae [24]. In 2022, a fractional mathematical model was used to study and investigate the dynamic behaviour of tuberculosis; the AB caputo and the fractional caputo have been contrasted [25]. In 2021, Dhiraj Kumar Das et al. studied the effectiveness of contact tracing in mitigating the COVID-19 outbreak [26]. Treatment optimization in a two-strain TB [27, 28].

Motivated by the preceding, we provide a (SWI_RI_DCR) mathematical framework. The two most crucial elements in preventing the disease from spreading are as follows: First, early diagnosis and antibiotic treatment are essential for a successful recovery. The second issue is the significance of maintaining good personal cleanliness and strong immunity for both sick and non-infected individuals by eating a nutritious diet, consuming herbs, and quitting smoking. To illustrate graphically, we employed the SCSC approach. The SCSC Technique is highly accurate and efficient, achieving spectral convergence with fewer computational resources. It provides global approximation using shifted Chebyshev polynomials, making it well-suited for boundary-value problems and non-linear systems. The method ensures numerical stability, handles boundary conditions effectively, and is adaptable to various mathematical models. The SCSC Technique has been widely utilized in various fields to model and analyze complex systems.

The present article is organized into the following sections: Section 1 covered a thorough overview of TB. The unique, exist, non-negative, and bounded of solutions, the stability of the model, and the reproduction number are

described in Section 2. We offer the sensitivity analysis in Section 3. section 4: The SCSC Technique is used to solve the desired model. Finally, we conclude the paper and have a discussion in Section 5.

2 Creation and analysis of the model

The model includes six nonlinear ordinary differential equations of first order and first degree. This model contains six epidemiological compartments: susceptible (S), infected under medical care (C), latent TB patients (I_R), active TB patients (I_D), infected without diagnosis (W), and recovered (R). The compartment S increases due to new births θ and decreases when individuals come into contact with infectious persons from the infected group W at a rate β transition into the undiagnosed infected category W. Individuals with strong immunity and good hygiene in the S category transition to the recovered group at rate (κ), as TB spreads quickly especially in those with weaker immunity and poor hygiene. Individuals from the W category transition into three infected compartments: I_R, I_D, C, at rates α, r and σ, respectively. These transitions represent the progression of undiagnosed infections into diagnosed categories, such as latent TB, active TB, and individuals under treatment. Individuals from the three infected categories I_R, I_D, C, at rates $\delta_1\kappa$, $\delta_2\kappa$ and $\delta_3\kappa$ respectively, transition into the R category after recovering from the disease. As κ increases, the rate of recovery δ_i becomes significantly faster. After starting treatment, individuals transition from the infected category I_D and W to the C category at rates π and r. Categories transition to death at a rate represented by the natural mortality rate τ. Initial conditions S_0, W_0, I_{R0}, I_{D0}, C_0 and R_0 define the population distribution at the start of the analysis. Every member of society has an identical natural death rate. The desired model includes two equilibrium cases, including an endemic equilibrium (EE) and a bacteria-free equilibrium (FE). These states are obtained by setting the system's right side equal to zero.

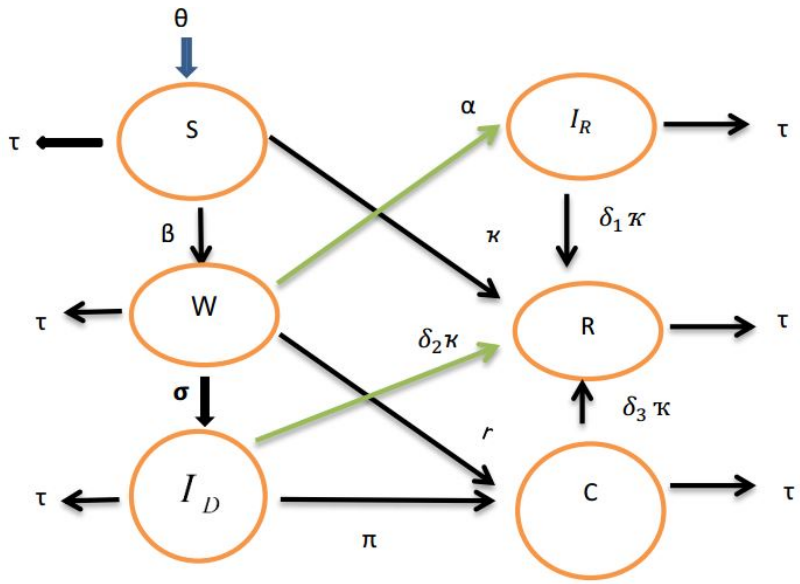

Fig. 1: Diagram showing the propagation of TB.

$$\begin{aligned}
\frac{dS}{dt} &= \theta - \beta WS - (\tau + \kappa)S \\
\frac{dW}{dt} &= \beta WS - (\alpha + \sigma + \tau + r)W \\
\frac{dI_R}{dt} &= \alpha W - \tau + \delta_1 \kappa)I_R \\
\frac{dI_D}{dt} &= \sigma W - (\pi + \tau + \delta_2 \kappa)I_D \\
\frac{dC}{dt} &= \pi I_D + rW - (\tau + \delta_3 \kappa)C \\
\frac{dR}{dt} &= \delta_1 \kappa I_R + \delta_2 \kappa I_D + \delta_3 \kappa C + \kappa S - \tau R
\end{aligned} \tag{1}$$

Table 1: The Biological interpretation of the symbols.

Symbols	Meaning
β	mixing rate
τ	death by natural causes
θ	human recruitment rate
$\delta_i, i = 1,2,3$	rate of recuperation
π	the rate of transmission to treatment
α	transfer rate from W to I_R
σ	transfer rate from W to I_D
r	early detection
κ	rate of personal hygiene and immune bolstering

Proposition 1. *$\Omega = \{(S,W,I_R,I_D,C,R) \in R^6 : 0 \leq N \leq \frac{\theta}{\tau}\}$ is a bounded region and the solutions set $\{S(t),W(t),I_R(t),I_D(t),C(t),R(t)\}$ of the model is positive and unique for all $t \geq 0$.*

Proof . Positivity of $[S(t),W(t),I_R(t),I_D(t),C(t),R(t)]$: The model equations can be represented as

$$\begin{aligned}
&\frac{dS}{dt} = \theta - \beta WS - \tau + \kappa)S \geqslant -BWS - \tau + \kappa)S, \\
&\frac{dW}{dt} \geqslant -(\alpha + \sigma + \tau + r)W, \\
&\frac{dI_R}{dt} \geqslant -(\tau + \delta_1 \kappa)I_R, \\
&\frac{dI_D}{dt} \geqslant -(\pi + \tau + \delta_2 \kappa)I_D, \\
&\frac{dC}{dt} \geqslant -(\tau + \delta_3 \kappa)C, \\
&\frac{dR}{dt} \geqslant -\tau R.
\end{aligned} \tag{2}$$

Integrating the two sides of Eq. (2) across the range $[0,t]$ yields the following result.

$$\begin{aligned}
&S(t) \geqslant S(0)e^{-(\beta \int_0^t W(x)dx + \tau t)}, \\
&W(t) \geqslant W(0)e^{-(\alpha+\sigma+\tau+r)t}, \\
&I_R(t) \geqslant I_R(0)e^{-(\tau+\delta_1 \kappa)t}, \\
&I_D(t) \geqslant I_D(0)e^{-(\pi+\tau+\delta_2 \kappa)t}, \\
&C(t) \geqslant C(0)e^{-(\tau+\delta_3 \kappa)t}, \\
&R(t) \geqslant R(0)e^{-\tau t},
\end{aligned} \tag{3}$$

exponential functions are always non-negative, regardless of the exponent's sign.

Simply $[S(t),W(t),I_R(t),I_D(t),C(t),R(t)]$ are positive for all $t \geqslant 0$.

Now, adding all the equations in model (1) yields

$$\frac{dN}{dt} = \theta - \tau N, \tag{4}$$

by performing the integration of the given Eq., upon integration and using the initial condition, the resulting expression is

$$N(t) = (N(0) - \frac{\theta}{\tau})e^{(-\tau t)} + \frac{\theta}{\tau}. \tag{5}$$

Therefore, it may be concluded that:

$$\lim_{t\to\infty} N(t) = \frac{\theta}{\tau}. \tag{6}$$

This demonstrates that N(t) is bounded within the range $0 \leq N(t) \leq \frac{\theta}{d}$, indicating that $\frac{\theta}{\tau}$ serves as the upper limit for N(t).

Now, we show that the system (1) has a unique solution.

Let the right-hand sides of the system (1) be represented below:

$$\begin{aligned}
G_1 &= \theta - \beta WS - (\tau+\kappa)S \\
G_2 &= BWS - (\alpha+\sigma+\tau+r)W \\
G_3 &= \alpha W - (\tau+\delta_1\kappa)I_R \\
G_4 &= \sigma W - (\pi+\tau+\delta_2\kappa)I_D \\
G_5 &= \pi I_D + rW - (\tau+\delta_3\kappa)C \\
G_6 &= \delta_1\kappa I_R + \delta_2\kappa I_D + \delta_3\kappa C + \kappa S - \tau R
\end{aligned} \tag{7}$$

Then the system (1) have a unique solution if $\frac{\partial G_n}{\partial V_m}$, $n,m = 1,2,3,4,5,6$ are continuous and bounded in Ω.

For G_1:

$$\begin{array}{lll}
|\frac{\partial G_1}{\partial S}| = |-(\beta W+\tau+\kappa)| < \infty; & |\frac{\partial G_1}{\partial W}| = |-(\beta S)| < \infty; & |\frac{\partial G_1}{\partial I_R}| = 0 < \infty; \\
|\frac{\partial G_1}{\partial I_D}| = 0 < \infty; & |\frac{\partial G_1}{\partial C}| = 0 < \infty; & |\frac{\partial G_1}{\partial R}| = 0 < \infty.
\end{array} \tag{8}$$

For G_2:

$$\begin{array}{lll}
|\frac{\partial G_2}{\partial S}| = |\beta W| < \infty; & |\frac{\partial G_2}{\partial W}| = |\beta S-(\alpha+\sigma+\tau+r)| < \infty; & |\frac{\partial G_2}{\partial I_R}| = 0 < \infty; \\
|\frac{\partial G_2}{\partial I_D}| = 0 < \infty; & |\frac{\partial G_2}{\partial C}| = 0 < \infty; & |\frac{\partial G_2}{\partial R}| = 0 < \infty.
\end{array} \tag{9}$$

For G_3:

$$\begin{array}{lll}
|\frac{\partial G_3}{\partial S}| = 0 < \infty; & |\frac{\partial G_3}{\partial W}| = |\alpha| < \infty; & |\frac{\partial G_3}{\partial I_R}| = -(\tau+\delta_1\kappa) < \infty; \\
|\frac{\partial G_3}{\partial I_D}| = 0 < \infty; & |\frac{\partial G_3}{\partial C}| = 0 < \infty; & |\frac{\partial G_3}{\partial R}| = 0 < \infty.
\end{array} \tag{10}$$

For G_4:

$$\begin{array}{lll}
|\frac{\partial G_4}{\partial S}| = 0 < \infty; & |\frac{\partial G_4}{\partial W}| = |\sigma| < \infty; & |\frac{\partial G_4}{\partial I_R}| = 0 < \infty; \\
|\frac{\partial G_4}{\partial I_D}| = |-(\pi+\tau+\delta_2\kappa)| < \infty; & |\frac{\partial G_4}{\partial C}| = 0 < \infty; & |\frac{\partial G_4}{\partial R}| = 0 < \infty.
\end{array} \tag{11}$$

For G_5:

$$\begin{array}{lll}
|\frac{\partial G_5}{\partial S}| = 0 < \infty; & |\frac{\partial G_5}{\partial W}| = r < \infty; & |\frac{\partial G_5}{\partial I_R}| = 0 < \infty; \\
|\frac{\partial G_5}{\partial I_D}| = |\pi| < \infty; & |\frac{\partial G_5}{\partial C}| = |-(\tau+\delta_3\kappa)| < \infty; & |\frac{\partial G_5}{\partial R}| = 0 < \infty.
\end{array} \tag{12}$$

For G_6:

$$\begin{array}{lll} |\frac{\partial G_6}{\partial S}| = |\kappa| < \infty; & |\frac{\partial G_6}{\partial W}| = 0 < \infty; & |\frac{\partial G_6}{\partial I_R}| = |\delta_1 \kappa| < \infty; \\ |\frac{\partial G_6}{\partial I_D}| = |\delta_2 \kappa| < \infty; & |\frac{\partial G_6}{\partial C}| = |\delta_3 \kappa| < \infty; & |\frac{\partial G_6}{\partial R}| = |-\tau| < \infty. \end{array} \tag{13}$$

This illustrates that all partial derivatives $\frac{\partial G_n}{\partial V_m}$, $n,m = 1,2,3,4,5,6$ exist, are continuous, and bounded in Ω. As a result, the Lipschitz criterion implies that system (1) admits a unique solution.

Now, the proof is complete.

To determine the system's equilibrium points, by taking

$$\frac{dS}{dt} = \frac{dW}{dt} = \frac{dI_R}{dt} = \frac{dI_D}{dt} = \frac{dC}{dt} = \frac{dR}{dt} = 0. \tag{14}$$

There are two equilibrium points FE and EE

$$FE = (S^0, W^0, I_R^0, I_D^0, C^0, R^0) = (\frac{\theta}{\tau+\kappa}, 0, 0, 0, 0, 0), \tag{15}$$

and

$$EE = (S^1, W^1, I_R^1, I_D^1, C^1, R^1), \tag{16}$$

where

$$\begin{array}{lll} S^1 = \frac{\alpha+\sigma+\tau+r}{\beta}, & W^1 = \frac{\theta-(\tau+\kappa)S^1}{\beta S^1}, & I_R^1 = \frac{\alpha W^1}{\tau+\delta_1\kappa}, \\ I_D^1 = \frac{\sigma W^1}{\pi+d+\delta_2\kappa}, & C^1 = \frac{\pi I_D^1 + r W^1}{\delta_3\kappa+\tau}, & R^1 = \frac{\delta_3\kappa C^1 + \delta_1\kappa I_R^1 + \delta_2\kappa I_D^1 + \kappa S^1}{\tau}. \end{array} \tag{17}$$

Definition 1. *The average total number of secondary cases caused by a single primary infection during an infectious outbreak is known as the basic reproduction number R_0, which is the largest absolute value of a next-generation matrix FH^{-1} [29]. this calculation is created using the classes W, I_R, I_D, C.*

Let

$$f = \begin{pmatrix} \beta SW \\ 0 \\ 0 \\ 0 \end{pmatrix}, h = \begin{pmatrix} (\alpha+\sigma+\tau+r)W \\ -\alpha W + (\tau+\delta_1\kappa)I_R \\ -\sigma W + (\pi+\tau+\delta_2\kappa)I_D \\ -\pi I_D - rW + (\tau+\delta_3\kappa)C \end{pmatrix}, \tag{18}$$

similar to reference [29], the Jacobian matrices of f and h at EF are represented as

$$F = \begin{pmatrix} \beta S^0 & 0 & 0 & 0 \\ 0 & 0 & 0 & 0 \\ 0 & 0 & 0 & 0 \\ 0 & 0 & 0 & 0 \end{pmatrix}, \tag{19}$$

$$H = \begin{pmatrix} \alpha+\sigma+\tau+r & 0 & 0 & 0 \\ -\alpha & \tau+\delta_1\kappa & 0 & 0 \\ -\sigma & 0 & \pi+\tau+\delta_2\kappa & 0 \\ -r & 0 & -\pi & \tau+\delta_3\kappa \end{pmatrix}, \tag{20}$$

$$FH^{-1} = \begin{pmatrix} \frac{\beta\theta}{(\tau+\kappa)(\alpha+\sigma+\tau+r)} & 0\,0\,0 \\ 0 & 0\,0\,0 \\ 0 & 0\,0\,0 \\ 0 & 0\,0\,0 \end{pmatrix}. \tag{21}$$

Furthermore, this basic reproduction number (R_0) is defined as follows:

$$R_0 = \frac{\beta\theta}{(\tau+\kappa)(\alpha+\sigma+\tau+r)}. \tag{22}$$

Lemma 1. *The model (1) has an endemic point, which exists if* $R_0 > 1$.

Proof . By using the value of R_0 with the value of EE point, we obtain

$$\begin{aligned} S^1 &= \tfrac{\alpha+\sigma+\tau+r}{\beta}, & W^1 &= \tfrac{(\tau+\kappa)(R_0-1)}{\beta}, \\ I_R^1 &= \tfrac{\alpha(\tau+\kappa)(R_0-1)}{\beta(\tau+\delta_1\kappa)}, & I_D^1 &= \tfrac{\sigma(\tau+\kappa)(R_0-1)}{B(\pi+\tau+\delta_2\kappa)}, \\ C^1 &= \tfrac{(d+\kappa)(R_0-1)}{\beta(\tau+\delta_3\kappa)}\left(\tfrac{\pi\sigma}{\pi+\tau+\delta_2\kappa}+r\right), & R^1 &= \tfrac{\kappa(R_0-1)}{\beta\tau}\left[(\tau+\kappa)\left(\tfrac{\delta_1\alpha}{\tau+\delta_1\kappa}+\tfrac{\delta_2\sigma}{\pi+\tau+\delta_2\kappa}+\tfrac{\delta_3\left(\frac{\pi\sigma}{\pi+\tau+\delta_2\kappa}\right)+r}{\tau+\delta_3\kappa}+\tfrac{\alpha+\sigma+\tau+r}{R_0-1}\right)\right]. \end{aligned} \tag{23}$$

It is clear that EE point is exit when $R_0 > 1$.

2.1 Study of stability

The Jacobian matrix as in [30–33] at any point of the SWI_RI_DCR system is

$$J = \begin{pmatrix} -\beta W-(\tau+\kappa) & -\beta S & 0 & 0 & 0 & 0 \\ \beta W & \beta S-(\alpha+\sigma+\tau+r) & 0 & 0 & 0 & 0 \\ 0 & \alpha & -(\tau+\delta_1\kappa) & 0 & 0 & 0 \\ 0 & \sigma & 0 & -(\pi+\tau+\delta_2\kappa) & 0 & 0 \\ 0 & r & 0 & \pi & -(\tau+\delta_3\kappa) & 0 \\ \kappa & 0 & \delta_1\kappa & \delta_2\kappa & \delta_3\kappa & -\tau \end{pmatrix}. \tag{24}$$

Theorem 1. *When* $R_0 < 1$ *the FE point is local stable.*

Proof . The Jacobian matrix evaluated at equilibrium $FE = (\frac{\theta}{\tau+\kappa}, 0,0,0,0,0)$ becomes

$$J_0 = \begin{pmatrix} -(\tau+\kappa) & -\beta S^0 & 0 & 0 & 0 & 0 \\ 0 & \beta S^0-(\tau+\sigma+r+\alpha) & 0 & 0 & 0 & 0 \\ 0 & \alpha & -(\tau+\delta_1\kappa) & 0 & 0 & 0 \\ 0 & \sigma & 0 & -(\pi+\tau+\delta_2\kappa) & 0 & 0 \\ 0 & r & 0 & \pi & -(\tau+\delta_3\kappa) & 0 \\ \kappa & 0 & \delta_1\kappa & \delta_2\kappa & \delta_3\kappa & -\tau \end{pmatrix}, \tag{25}$$

in this matrix, the eigenvalues are $-(\tau+\kappa), -(\tau+\delta_1\kappa), -(\pi+\tau+\delta_2\kappa), -(\tau+\delta_3\kappa), -\tau$ and $\beta S^0-(\tau+\sigma+r+\alpha)$. Since $\beta S^0-(\tau+\sigma+r+\alpha)=(\tau+\sigma+r+\alpha)(R_0-1)$, When $R_0<1$, the eigenvalue is negative, joining the preceding five negative eigenvalues. Evidently, FE point is locally asymptotically stable when $R_0<1$ and unstable otherwise.

Theorem 2. *The FE point of SWI_RI_DC model is global asymptotically stable whenever $R_0<1$ and unstable otherwise.*

Proof . A Lyapunov function defined as $L=W$,

$$\frac{dL}{dt}=\frac{dW}{dt}=BWS-(\alpha+\sigma+d+r)W\leq W[BS^0-(\alpha+\sigma+d+r)], \tag{26}$$

it follows that

$$\frac{dL}{dt}\leq W[\alpha+\sigma+\tau+r](R_0-1). \tag{27}$$

It is obvious that $\frac{dL}{dt}<0$ in case $R_0<1$ and $\frac{dL}{dt}>0$ in case $R_0>1$. In addition, $\frac{dL}{dt}=0$ if and only if $W=0$, It is shown that it is equal to zero at FE. Therefore, By LaSalle"s extension to Lyapunov's principle [44– 47], E_0 is globally asymptotically stable when $R_0<1$ and unstable when $R_0>1$.

Theorem 3. *The EE point of $SWI_R\,I_DCR$ model is local asymptotically stable when $R_0>1$.*

Proof . The Jacobian matrix evaluated at equilibrium $EE=(S^1,W^1,I_R^1,I_D^1,C^1,R^1)$ becomes

$$J_{EE}=\begin{pmatrix} -\beta W^1-(\tau+\kappa) & -\beta S^1 & 0 & 0 & 0 & 0\\ \beta W^1 & \beta S^1-(\alpha+\sigma+\tau+r) & 0 & 0 & 0 & 0\\ 0 & \alpha & -(\tau+\delta_1\kappa) & 0 & 0 & 0\\ 0 & \sigma & 0 & -(\pi+\tau+\delta_2\kappa) & 0 & 0\\ 0 & r & 0 & \pi & -(\tau+\delta_3\kappa) & 0\\ \kappa & 0 & \delta_1\kappa & \delta_2\kappa & \delta_3\kappa & -\tau \end{pmatrix}, \tag{28}$$

now, the eigenvalues of J_{EE} are requisite to be created. The characteristic equation $\det|J_{EE}-\lambda I|=0$

Clearly, there are four negative eigenvalues $\lambda_1=-(\tau+\delta_1\kappa)$, $\lambda_2=-(\pi+\tau+\delta_2\kappa)$, $\lambda_3=-(\tau+\delta_3\kappa)$, $\lambda_4=-\tau$, and other eigenvalues satisfy the quadratic equation

$$b\lambda^2+c\lambda+d=0,$$

where

$$b=1,$$
$$c=-\beta S^1+\alpha+\sigma+\tau+r+\tau W^1+\tau+\kappa,$$
$$d=\beta W^1(\alpha+\sigma+\tau+r)-(\tau+\kappa)\beta S^1+(\tau+\kappa)(\alpha+\sigma+\tau+r).$$

The Routh-Hurwitz criterion [32], [33] is used to find the signs of the solutions, or eigenvalues, of the characteristic equation. The Routh-Hurwitz criteria indicate that EE is locally asymptotically stable when three conditions are satisfied.

(1) $b>0$ (2) $c>0$ (3) $d<0$.

Evidently, $b>0$, $c>0$ and $d<0$. Hence EE point is LAS.

Theorem 4. *The EE point of SWI_R I_DCR model is global asymptotically stable when $R_0 > 1$.*

Proof . utilizing the lyapunov function, the endemic equilibrium point's global stability is investigated.

The lyapunov function can be choosing as:

$$L = \frac{1}{2}((S-S^1)+(W-W^1)+(I_R-I_R^1)+(I_D-I_D^1)+(C-C^1)+(R-R^1))^2, \tag{29}$$

thus, it indicates that

$$\begin{aligned}\frac{dL}{dt} &= ((S-S^1)+(W-W^1)+(I_R-I_R^1)+(I_D-I_D^1)+(C-C^1)+(R-R^1))(\frac{dS}{dt}+\frac{dW}{dt}+\frac{dI_R}{dt}+\frac{dI_D}{dt}+\frac{dC}{dt}+\frac{dR}{dt})\\ &= (N-\frac{\theta}{\tau})(\theta-\tau N) = -\frac{(\theta-\tau N)^2}{\tau} < 0.\end{aligned} \tag{30}$$

As a result, $\frac{dL}{dt} < 0$ suggests that the function is lyapunov. It is obvious that $\frac{dL}{dt} = 0$ when $S = S^1, I_D = I_D^1, W = W^1, C = C^1, I_R = I_R^1$ and $R = R^1$, indicating that EE point is global asymptotic stability.

3 Analysis of parameter sensitivity

In epidemiology, the sensitivity analysis is crucial and especially in mathematical modeling of infectious disease. we performed a multivariate sensitivity analysis of the model in order to identify the most important parameters for the control of the epidemic. It displays the impact of the model's parameters on the fundamental reproduction number [34]. the positive values of the sensitivity parameters means that there is direct relationship and the negative sign is an inverse relationship. R_0's sensitivity to α is described as

$$S_\alpha^{R_0} = \frac{\alpha}{R_0} \times \frac{\partial R_0}{\partial \alpha}, \tag{31}$$

similarly, we estimate the other parameters' sensitivity B, θ, d, r and κ are as follows:

$$S_B^{R_0} = 1 > 0, \tag{32}$$

$$S_\theta^{R_0} = 1 > 0, \tag{33}$$

$$S_d^{R_0} = \frac{-d(\alpha+\sigma+2d+\kappa+r)}{(d+\kappa)(\alpha+\sigma+d+r)} < 0, \tag{34}$$

$$S_\sigma^{R_0} = \frac{-\sigma}{(\alpha+\sigma+d+r)} < 0, \tag{35}$$

$$S_\alpha^{R_0} = \frac{-\alpha}{(\alpha+\sigma+d+r)} < 0, \tag{36}$$

$$S_\kappa^{R_0} = \frac{-\kappa}{d+\kappa} < 0, \tag{37}$$

$$S_r^{R_0} = \frac{-r}{(\alpha+\sigma+d+r)} < 0. \tag{38}$$

The computations above and Figure (2) indicate that R_0 rises with an increase in B and θ and while it decreases as τ, r, κ, σ and α grow. This highlights the sensitivity of R_0 to these parameters, emphasizing their role in controlling the spread of infection.

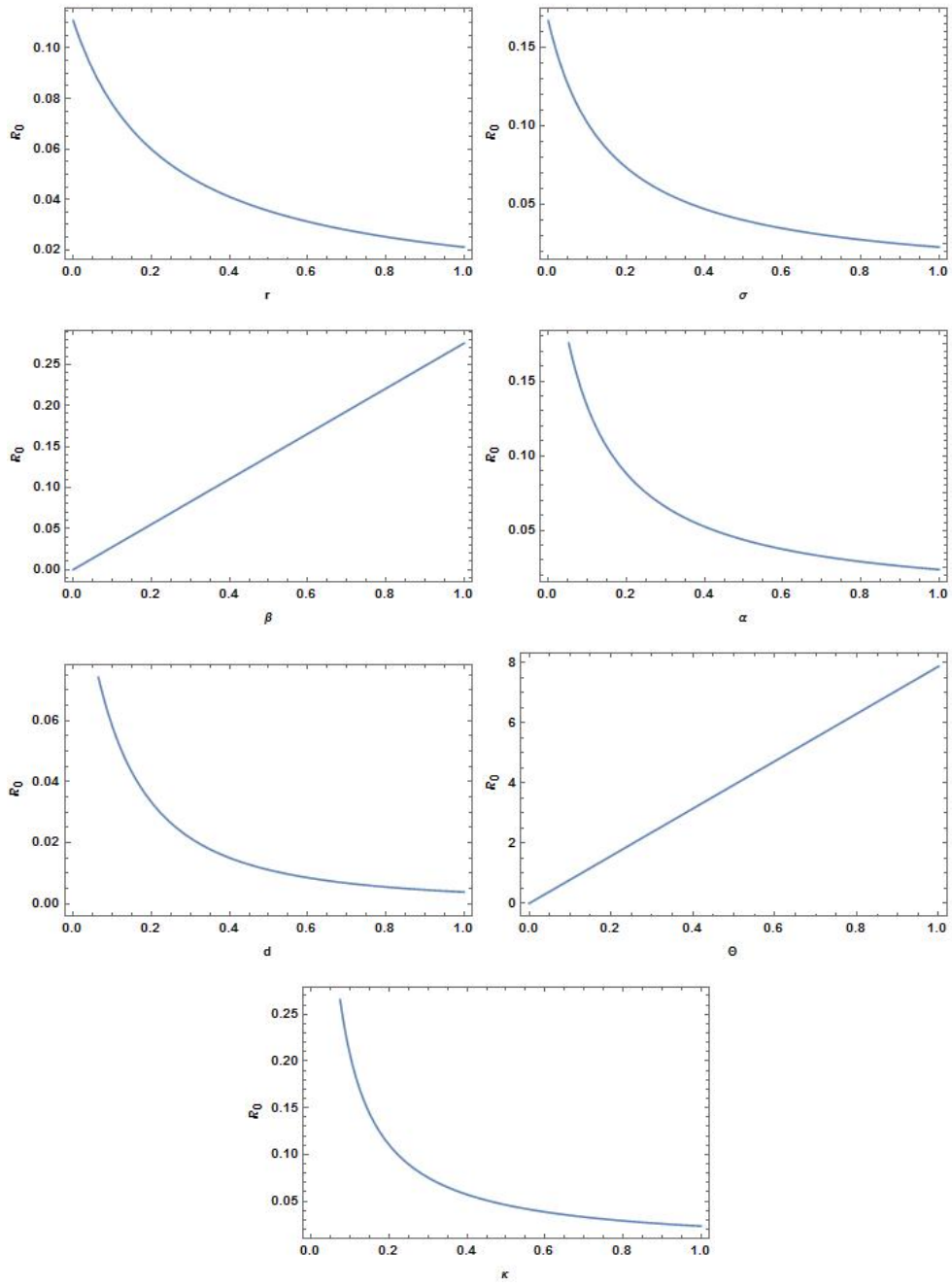

Fig. 2: Parameter sensitivity indices.

4 Solving the model with SCSC technique

To clarify the SCSC technique, first, we offer the recurrence formula that can be used to determine the Chebyshev polynomials as in [35], which determined on the range $[-1,1]$ as

$$T_{m+1}(y) = 2yT_m(y) - T_{m-1}(y), \quad T_0(y) = 1, \quad T_1(y) = y, \quad m = 1,2,... \tag{39}$$

It is understood that $T_m(-1) = (-1)^m$, $T_m(1) = 1$.The Chebyshev polynomials $T_m(y)$ of degree m have analytic form:

$$T_m(y) = \sum_{s=0}^{[m/2]} (-1)^s 2^{m-2s-1} \frac{m(m-s-1)!}{(s)!(m-2s)!} y^{m-2s}, \tag{40}$$

where $[m/2]$ represents the integer component of $m/2$. When orthogonality exists,

$$\int_{-1}^{1} \frac{T_s(y)T_j(y)}{\sqrt{1-y^2}} dy = \begin{cases} \pi, \ for s = j = 0; \\ \frac{\pi}{2}, \ for s = j \neq 0; \\ 0, \ for s \neq j. \end{cases} \tag{41}$$

By changing the variable $y = \frac{2x}{L} - 1$, we define shifted Chebyshev polynomials, which can be used on the interval $[0,L]$. Because of this, there is a description of the shifted Chebyshev polynomials as $T_m^*(x) = T_m(\frac{2x}{L} - 1) = T_{2m}(\sqrt{\frac{x}{L}})$. $T_m^*(x)$ of degree m has the following analytic form

$$T_m^*(x) = m \sum_{k=0}^{m} (-1)^{m-k} \frac{(m+k-1)!2^{2k}}{(m-k)!(2k)!L^k} x^k, \qquad m = 2,3,... \tag{42}$$

where, $T_m^*(L) = 1$, $T_m^*(0) = (-1)^m$ These polynomials' orthogonality condition is

$$\int_0^L T_k^*(x) w(x) T_j^*(x) dx = \delta_{jk} b_k, \tag{43}$$

the weight function as $w(x) = \frac{1}{\sqrt{Lx-x^2}}$, $b_k = \frac{h_k}{2}\pi$, with $h_0 = 2$, $h_k = 1$, $k \geqslant 1$.The square integrabel function defined in [0, L], $Z(x)$ can be represented as shifted Chebyshev polynomials.

$$Z(x) = \sum_{m=0}^{\infty} c_m T_m^*(x), \tag{44}$$

where the coefficients c_m are defined as follows

$$c_m = \frac{1}{b_m} \int_0^L w(x) Z(x) T_m^*(x) dx, \qquad m = 0,1,... \tag{45}$$

to find the model's numerical solution. We first provide a convergence analysis of the suggested formula.

Theorem 5. *The error in approximating X(t) by the sum of its first z terms is bounded by the sum of the absolute values of all the neglected coefficients [35]. If*

$$X_z(t) = \sum_{k=0}^{z} c_k T_k(t), \tag{46}$$

$$E_T(z) = |X(t) - X_z(t)| \leq \sum_{k=z+1}^{\infty} |c_k|,\ t \in [-1,1]. \tag{47}$$

To solve the model using the SCSC method. The main steps of the procedure solution can be summarized as follows

Step 1 : we first approximation $S(t), W(t), I_R(t), I_D(t), C(t)$ and $R(t)$ as.

$$S_h(t) = \sum_{m=0}^{h} a_m T_m^*(t), \tag{48}$$

$$W_h(t) = \sum_{m=0}^{h} b_m T_m^*(t), \tag{49}$$

$$I_{Rh}(t) = \sum_{m=0}^{h} c_m T_m^*(t), \tag{50}$$

$$I_{Dh}(t) = \sum_{m=0}^{h} d_m T_m^*(t), \tag{51}$$

$$C_h(t) = \sum_{m=0}^{h} e_m T_m^*(t), \tag{52}$$

$$R_h(t) = \sum_{m=0}^{h} f_m T_m^*(t), \tag{53}$$

where a_m, b_m, c_m, d_m, e_m and f_m are constants to be determined. By applying this approximation to the SWI_RI_DCR model we obtain

$$\begin{gathered}
\textstyle\sum_{m=0}^{h} a_m T_m^{'*}(t) = \theta - B\sum_{m=0}^{h} b_m T_m^*(t) \sum_{m=0}^{h} a_m T_m^*(t) - [d+\kappa]\sum_{m=0}^{h} a_m T_m^*(t), \\
\textstyle\sum_{m=0}^{h} b_m T_m^{'*}(t) = B\sum_{m=0}^{h} b_m T_m^*(t) \sum_{m=0}^{h} a_m T_m^*(t) - [\alpha+\sigma+d+r]\sum_{m=0}^{h} b_m T_m^*(t), \\
\textstyle\sum_{m=0}^{h} c_m T_m^{'*}(t) = \alpha\sum_{m=0}^{h} b_m T_m^*(t) - [d+\delta_1\kappa]\sum_{m=0}^{h} c_m T_m^*(t), \\
\textstyle\sum_{m=0}^{h} d_m T_m^{'*}(t) = \sigma\sum_{m=0}^{h} b_m T_m^*(t) - (\pi+d+\delta_2\kappa)\sum_{m=0}^{h} d_m T_m^*(t), \\
\textstyle\sum_{m=0}^{h} e_m T_m^{'*}(t) = \pi\sum_{m=0}^{h} d_m T_m^*(t) + r\sum_{m=0}^{h} b_m T_m^*(t) - (d+\delta_3\kappa)\sum_{m=0}^{h} e_m T_m^*(t), \\
\textstyle\sum_{m=0}^{h} f_m T_m^{'*}(t) = \kappa\delta_1\sum_{m=0}^{h} c_m T_m^*(t) + \kappa\delta_2\sum_{m=0}^{h} d_m T_m^*(t) + \kappa\delta_3\sum_{m=0}^{h} e_m T_m^*(t) + \kappa\sum_{m=0}^{h} a_m T_m^*(t) \\
\textstyle -d\sum_{m=0}^{h} f_m T_m^*(t),
\end{gathered} \tag{54}$$

for m=0, 1, ..., h, the initial conditions give the following equations

$$\begin{gathered}
\textstyle\sum_{m=0}^{h}(-1)^m a_m = S_0, \qquad \sum_{m=0}^{h}(-1)^m b_m = W_0, \qquad \sum_{m=0}^{h}(-1)^m c_m = I_{R0}, \\
\textstyle\sum_{m=0}^{h}(-1)^m d_m = I_{D0}, \qquad \sum_{m=0}^{h}(-1)^m e_m = C_0, \qquad \sum_{m=0}^{h}(-1)^m f_m = R_0.
\end{gathered} \tag{55}$$

Step 2 : Collocate Eq.(54) at the $6h$ points. For an appropriate collocation points, apply SCSC roots T_h^*.
Step 3 : An algebraic system is represented by the equations derived in step 2 and the initial conditions with 6(h+1) of unknowns.

The numerical solutions obtained by the SCSC method show the spread of the virus among the general public. Mathematica 11 was used to create all of the codes. The trajectory of the approximate solution with h = 8 is illustrated.

Table 2: The model's parameters expressed numerically

Symbols	Estimator	Citation
B	0.4	approximations
d	0.015	approximations
A	0.014	[36]
δ_i, i=1,2,3	0.4038	[37]
θ	0.014	approximations
α	0.14	[37], [38]
σ	0.08	approximations
r	0.001	approximations
κ	0.2	approximations

Firstly, Figure 3 presents six sub figures that model the dynamics of a community segmented into compartments: S, W, I_R, I_D, C, R. This visualization examines the effects of robust immunity and improved personal hygiene on both the individuals in these compartments and the overall disease spread within the community. To investigate these effects, the model evaluates four distinct values for the parameter κ. The value of κ is varied while all other parameters remain constant. Strong immunity and good personal hygiene have a positive impact on society members, as figure 3 illustrates. As we investigate the line graphs with various κ values, as noted in Figures 3(a), 3(b), 3(c), 3(d), and 3(e), the number of susceptible, latent TB patients, infected without diagnosis, infected under medical care and people with active TB declines as κ increases. Initially, when $\kappa = 0.005$ gives $R_0 = 1.19$ and when $\kappa = 0.1$ gives $R_0 = 0.2$. The spread of TB has no influence on the human population when the reproduction number is significantly smaller than one because there aren't many susceptible. We observe that by increasing the value of κ, the number of recoveries increases, as immunity plays a crucial role in speeding up recovery, as shown in Figure 3(f).

Secondly, Figure 4 illustrates the influence of the parameter r, which represents the early detecting rate, while keeping all other parameters constant. As is apparent in Figure 4(a) there impact is minimal of early detection on susceptible people. The early detection becomes evident in Figures 4(b), 4(c), and 4(d), which detail the dynamics of infected populations and disease progression. Specifically, Figure 4(b) shows a notable reduction in the population of undiagnosed infected individuals, whereas Figure 4(c) illustrates a decline in the number of individuals with latent TB. Figure 4(d) further demonstrates a substantial decrease in the population of those with active TB, with these numbers approaching zero over time. Thus, early detection has an important impact due to a decrease in the number of infected and moreover, a rise in the number of recovered.

The findings emphasize that early detection plays a critical role in curbing TB spread. By identifying infections in their latent or early stages, effective interventions, such as timely treatment and isolation, can be implemented to prevent progression to active TB and subsequent transmission.

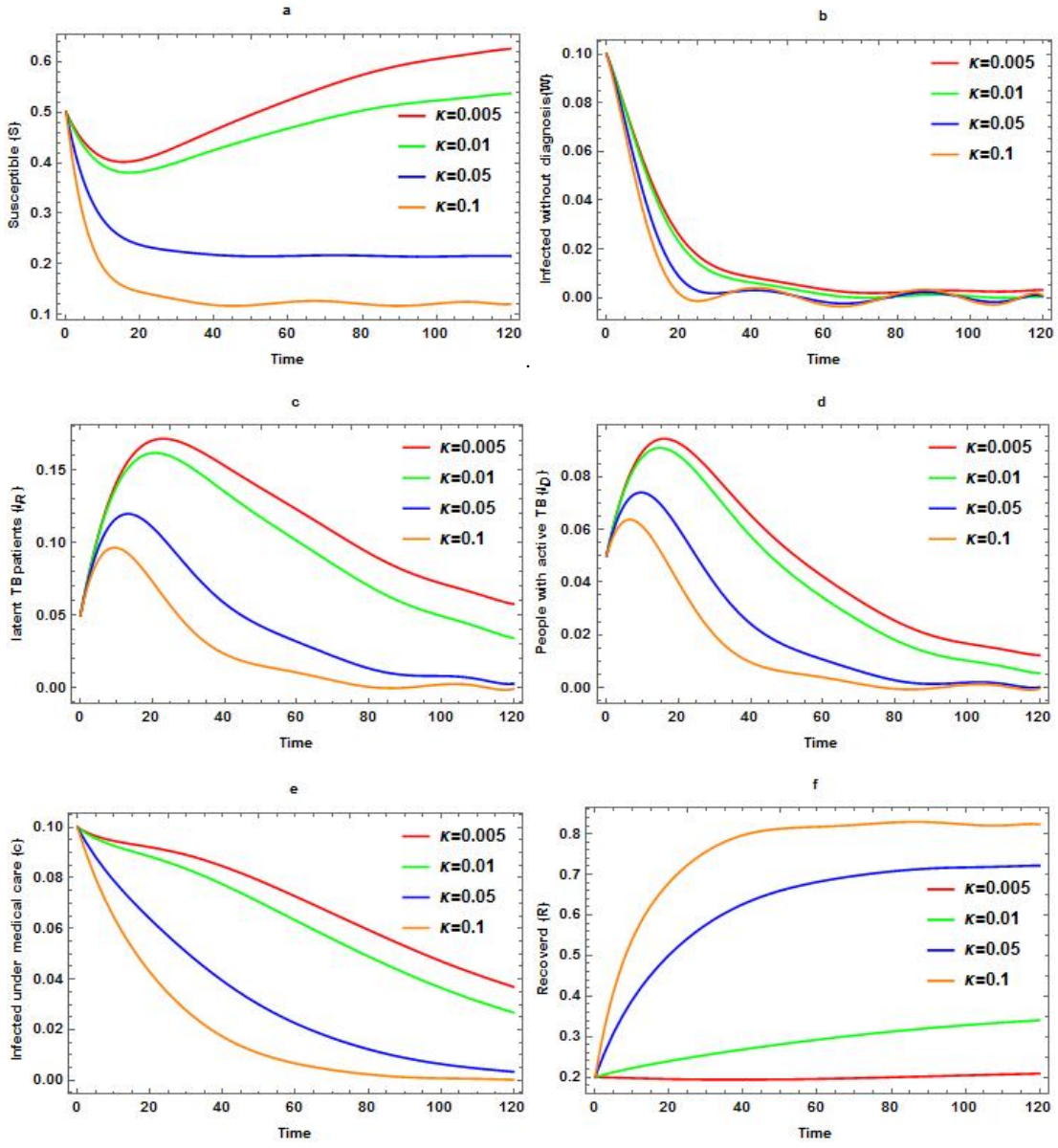

Fig. 3: S, W, I_R, I_D, C and R trajectories for multiple values of κ.

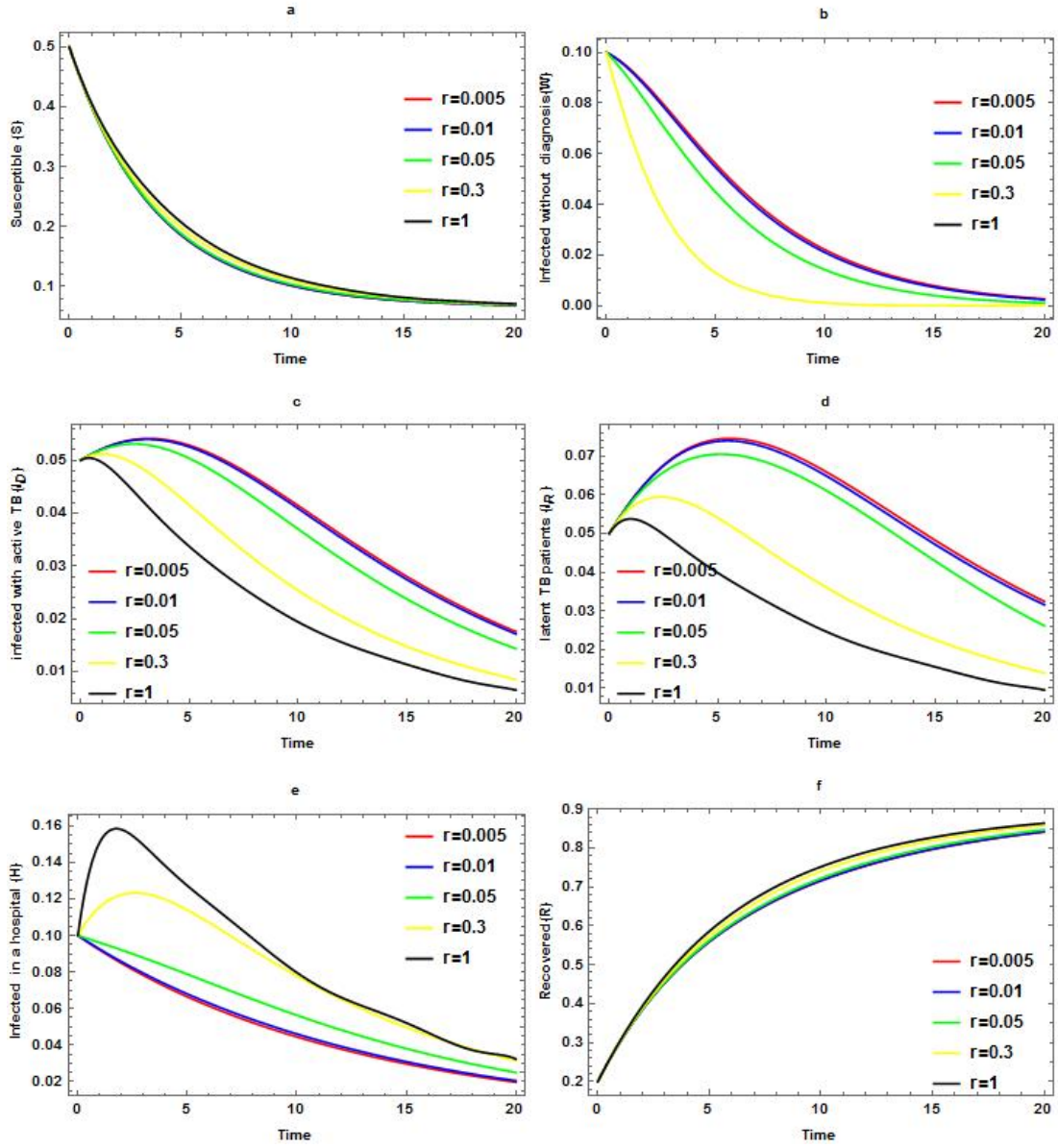

Fig. 4: S, W, I_R, I_D, C and R trajectories for multiple values of r.

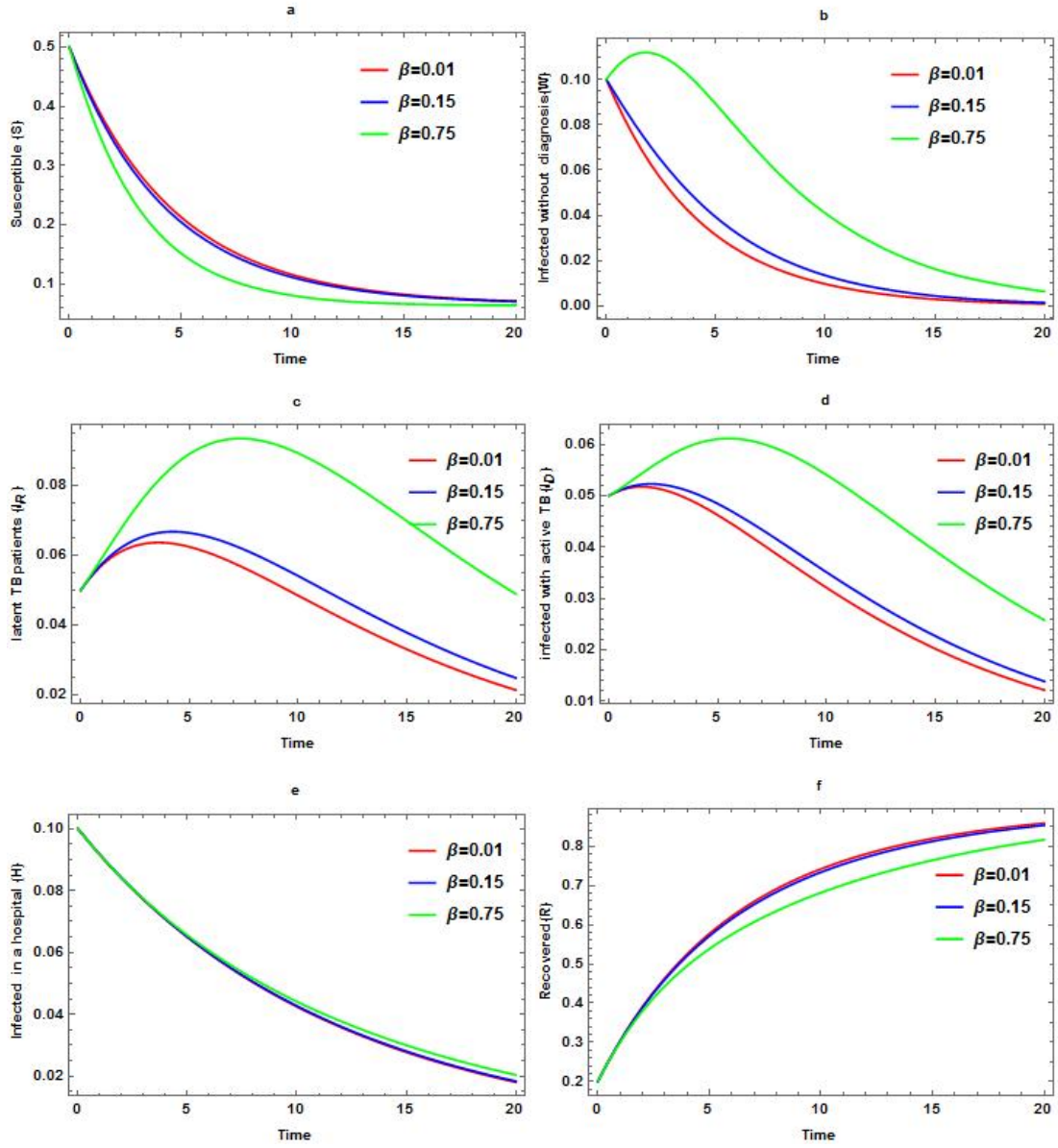

Fig. 5: S, W, I_R, I_D, C and R trajectories for multiple values of B.

Figure 5 shows how important the contact rate (β), in shaping the disease's dissemination among different demographic subsets with increasing time. Figure (a) specifically shows how the contact rate affects susceptible individuals. We observe that as the value of β increases, the number of susceptible individuals decreases, as these individuals transition into the infected categories. Consequently, the number of recovered individuals also reduces, as fewer individuals remain in the susceptible group or recover directly. A significant and noticeable increase in

the three categories, numbered W, I_R and I_D as represented in Figures 5(b), 5(c) and 5(d). In contrast to the C class, its value increases only slightly with the increase in parameters, as shown in Figure 5(e).

5 Conclusions and remarks

We have developed and studied a numerical representation of TB. A class of SIR modeling with vital behavior and a bounded community is shown. We developed the SWI_RI_DCR model to concentrate on the importance of immunity, personal hygiene, and early detection after first reviewing a few recently published articles and articles that worked on TB. The biological significance of the model is illustrated through the existence of a unique, non negative, and bounded solution within a specific domain. Two steady-state points for the model were calculated with and without the TB. An endemic point exists if $R_0 > 1$ and is global and local stable. According to stability, for $R_0 < 1$, the bacteria-free equilibrium (FE) was both locally and globally asymptotically stable. Graphic illustrations and numerical and sensitivity analyzes verify that early detection, good personal hygiene, and strong immunity will all contribute to reducing TB transmission. Furthermore, the simulation result clarifies that while a decrease in effective contact rates and an increase in treatments would minimize the globalization of TB, an increase in contact rate made the disease worse. For finding the numerical solutions, the Chebyshev spectral collocation SCSC technique was applied. Finally, the versatility of the proposed model allows it to be adapted to other infectious diseases, broadening its applicability beyond TB and contributing to a generalized framework for studying disease transmission dynamics.

Availability of data and material

Data sharing is not applicable to this article as no datasets were generated or analyzed during the current study.

Conflict of interest

The author declares that the have no competing interests.

Funding

There is no funding source for the research.

Authors' contributions

The authors contribute equally to the work.

Acknowledgment

The author would like to thank anonymous reviewers.

References

[1] A. Atangana, S. Qureshi, Mathematical modeling of an autonomous nonlinear dynamical system for malaria transmission using Caputo derivative, in *Fractional Order Analysis*, 225–252 (2020).

[2] O.J. Peter, A.S. Shaikh, M.O. Ibrahim, K.S. Nisar, D. Baleanu, I. Khan, A.I. Abioye, Analysis and dynamics of fractional order mathematical model of Covid-19 in Nigeria using Atangana–Baleanu operator, *Comput. Mater. Continua*, **66**, 1823–1848 (2021).

[3] O.J. Peter, S. Qureshi, A. Yusuf, M. Al-Shomrani, A.A. Idowu, A new mathematical model of Covid-19 using real data from Pakistan, *Results Phys.*, **24**, 104098 (2021).

[4] H. Khan, J. Gómez-Aguilar, A. Khan, A. Alkhazzan, A fractional order HIV-TB coinfection model with nonsingular Mittag–Leffler law, *Math. Methods Appl. Sci.*, **43**(6), 3786–3806 (2020).

[5] P.U. Madueme, F. Chirove, A systematic review of mathematical models of Lassa fever, *Math. Biosci.*, **374**, 109227 (2024).

[6] Y. Naik, V. Kumar, M. Naik, Review of mathematical models for tuberculosis with reference to India, *J. Nonlinear Anal. Optim.*, **15**(2) (2024).

[7] S. Ullah, O. Ullah, M. Khan, T. Gul, Sensitivity analysis of dengue model with saturated incidence rate, *Eur. Phys. J. Plus*, **602**(135), 8–27 (2020).

[8] H. Badawi, N. Shawagfeh, O. Abu Arqub, Fractional Conformable Stochastic Integrodifferential Equations: Existence, Uniqueness, and Numerical Simulations Utilizing the Shifted Legendre Spectral Collocation Algorithm, *Math. Probl. Eng.*, (2022).

[9] B. Maayah, O. Abu Arqub, S. Alnabulsi, H. Alsulami, Existence, uniqueness, and galerkin shifted Legendre's approximation of time delays integrodifferential models by adapting the Hilfer fractional attitude, *Heliyon*, **10**(4), 2405-8440 (2024).

[10] N. Ahmed, S.E. Hasnain, Molecular epidemiology of tuberculosis in India: moving forward with a systems biology approach, *Tuberculosis (Edinb)*, **91**, 407–413 (2011).

[11] I. Ullah, Q. Ahmad, S. Al-Mdallal, Z. Khan, H. Khan, A. Khan, Stability analysis of a dynamical model of tuberculosis with incomplete treatment, *Adv. Differ. Equ*, **1**, 1–14 (2020).

[12] I. Syahrini, Sriwahyuni, V. Halfiani, S.M. Yuni, Rasudin, T. Iskandar, M. Ramli, The epidemic of tuberculosis on vaccinated population, *J. Phys. Conf. Ser*, **890**(1), 1–5 (2017).

[13] J. Liu, T. Zhang, Global stability for a tuberculosis model, *Math. Comput. Model*, **54**(1), 836–845 (2011).

[14] J. Andrawus, F.Y. Eguda, I.G. Usman, S.I. Maiwa, I. Dibal, T. Urum, G. Anka, A mathematical model of a tuberculosis transmission dynamics incorporating first and second line treatment, *J. Appl. Sci. Environ. Manag*, **24**(5), 917–922 (2020).

[15] K. Selain, F. Emile, H. Vinh, Analysis and simulation of a mathematical model of tuberculosis transmission in Democratic Republic of the Congo, *Adv. Differ. Equ*, **642**, 1–19 (2020).

[16] S. Bowong, J.J. Tewa, Global analysis of a dynamical model for transmission of tuberculosis with a general contact rate, Commun. *Nonlinear Sci. Numer. Simul*, **15**, 3621–3631 (2010).

[17] H. Waaler, A. Geser, S. Andersen, The use of mathematical models in the study of the epidemiology of tuberculosis, *Am. J. Public Health Nation's Health*, **52**, 1002–1013 (1962).

[18] D. Greenhalgh, Some results for a SEIR epidemic model with density dependence in the death rate, *IMA J Math Appl Med Biol*, **9**, 67–106 (1992).

[19] K. Cooke, P. van den Driessche, Analysis of an SEIRS epidemic model with two delays, *J Math Biol*, **35**, 240–260 (1996).

[20] D. Greenhalgh, Hopf bifurcation in epidemic models with a latent period and nonpermanent immunity Model, *Math Comput*, **25**, 85–107 (1997).

[21] J. Zhang, Z. Ma, Global dynamics of an SEIR epidemic model with saturating contact rate, *Math Biosci*, **185**, 15–32 (2003).

[22] M. Y. Li, H. L. Smith, L. Wang, Global dynamics of an SEIR epidemic model with vertical transmission, *SIAM J Appl Math*, **62**, 58–69 (2001).

[23] H.F. Hou, M.X. Zou, Modelling effects of treatment at home on tuberculosis transmission dynamics Model, *Appl Math*, **40**, 9474–9484 (2016).

[24] D. Okuonghae, A mathematical model of tuberculosis transmission with heterogeneity in disease susceptibility and progression under a treatment regime for infectious cases, *Appl. Math. Model*, **37**(10), 6786–6808 (2013).

[25] Z. Zain Ul Abadin, Z. Sumera, H. M. Tanveer, T. Cemil, J. Shumaila, Analysis and numerical simulation of tuberculosis model using different fractional derivatives, *Chaos, Solitons and Fractals*, **160**, 112202 (2022).

[26] D. K. Das, A. Khatua, T. K. Kar, S. Jana, The effectiveness of contact tracing in mitigating COVID-19 outbreak: A model-based analysis in the context of India, *Applied Mathematics and Computation*, **404**, 126207 (2021).

[27] P. Van den Driessche, Reproduction numbers of infectious disease models, *Infectious Disease Modelling*, **2**(3), 288–303(2017).
[28] I. Ahmed, G. U. Modu, A. Yusuf, P. Kumam, I. Yusuf, A mathematical model of coronavirus disease (COVID-19) containing asymptomatic and symptomatic classes, *Results Phys*, **21**, 03776 (2021).
[29] J. Zhang, Y. Wang, and Z. Li, Dynamics and calculation of the basic reproduction number for a nonlocal dispersal epidemic model with air pollution, *J. Appl. Math. Comput.*, **69**, 3205–3229 (2023).
[30] J.P. LaSalle, The stability of dynamical systems, *CBMS-NSF Regional Conference Series in Applied Mathematics*, **25**, SIAM, Philadelphia (1976).
[31] G. Paul, Stability, Instability and Chaos An Introduction to the Theory of Nonlinear Differential Equations, *Cambridge Texts in Applied Mathematics*, (1994).
[32] W.R. Derrick, S.I. Grossman, Elementary differential equations with applications, *Addison-Wesley Ser. Math.*, (1976).
[33] D.K. Arrowsmith, C.M. Place, Ordinary differential equations, *series 2. Chapman and Hall*, **26**, 287-288 (1983).
[34] N. Chitnis, J. M. Hyman, J. M. Cushing, Determining important parameters in the spread of malaria through the sensitivity analysis of a mathematical model, *Bulletin of Mathematical Biology*, **70** (5), 1272–1296 (2008).
[35] M. A. Snyder, Chebyshev Methods in Numerical Approximation, Prentice-Hall, *Inc.: Englewood Cliffs, NJ, USA*, (1966).
[36] K. Cooke, P. van den Driessche, Analysis of an SEIRS epidemic model with two delays, *J. Math. Biol.*, **35**, 240–260 (1996).
[37] D. K. Das, T.K. Kar, Global dynamics of a tuberculosis model with sensitivity of the smear microscopy, *Chaos, Solitons and Fractals*, **(146)**, 0960-0779(2021).
[38] D.W. Dowdy, C. Dye, T. Cohen, Data needs for evidence-based decisions: a tuberculosis modeler's 'wish list' Int J Tuberc Lung Dis, **17** (7), 866-877 (2013).